SUPPLEMENTAL MATERIALS

Recurrent *YAP1-MAML2* and *YAP1-NUTM1* fusions in poroma and porocarcinoma

Shigeki Sekine, Tohru Kiyono, Eijitsu Ryo, Reiko Ogawa, Susumu Wakai, Hitoshi Ichikawa, Koyu Suzuki, Satoru Arai, Koji Tsuta, Mitsuaki Ishida, Yuko Sasajima, Naoki Goshima, Naoya Yamazaki, Taisuke Mori

- Supplemental Methods
- Supplemental Figures 1-5
- Supplemental Tables 1-3, 6, 7

Supplemental Methods

Tissue samples

The present study analyzed a total of 213 formalin-fixed paraffin-embedded (FFPE) specimens of skin tumors, including 104 poromas, 11 porocarcinomas, 24 squamous cell carcinomas, 32 basal cell carcinomas, 5 cutaneous adenocarcinomas, 9 Merkel cell carcinomas, and 27 seborrheic keratoses, obtained by surgical resection or biopsy at the National Cancer Center Hospital, Tokyo, Japan; St. Luke's International Hospital, Tokyo, Japan; Kansai Medical University Hospital, Osaka, Japan; or Teikyo University Hospital, Tokyo, Japan. Poromas included the following histological subtypes: 91 poromas, 5 hidroacanthoma simplex, 2 dermal duct tumors, and 6 poroid hidradenomas. Tumors with combined features were classified according to the predominant histological component. The presence of coagulative necrosis was also recorded.

Targeted next-generation RNA sequencing

Sections of FFPE samples were deparaffinized and subjected to RNA extraction using an RNeasy FFPE kit (Qiagen, Hilden, Germany). RNA sequencing was performed using the TruSight Pan-Cancer panel (Illumina, San Diego, CA, USA), which targets 1385 cancer-related genes, following manufacture's instruction. Sequencing was performed on the MiSeq (Illumina) using MiSeq Reagent Kit v3 150 cycles (Illumina). The fusion gene identification was performed using the RNA-Seq Alignment application (Illumina). The sequencing data are available in the Japanese Genotype-Phenotype Archive (JGA; https://trace.ddbj.nig.ac.jp/jga/) under the accession number JGAS00000000195.

RT-PCR

The reverse transcription reaction was performed using the high-capacity cDNA reverse transcription kit (ThermoFisher Scientific, Waltham, MA, USA). cDNA sample quality was assessed by PCR amplification of a 220-base pair fragment of *ACTB*. The primers were designed to amplify the fusion junctions detected by next-generation sequencing, or possible fusion junctions predicted from the exon structures of *YAP1*, *MAML2*, and *NUTM1* (Supplemental Table 6). Poromas and porocarcinomas were analyzed for all primer sets, whereas other skin tumors were examined using primer

sets detecting recurrent fusions. All PCR products were subjected to Sanger sequencing for confirmation. When required, the PCR products were subcloned using a TOPO TA cloning kit (ThermoFisher Scientific) prior to sequencing.

Fluorescent *in-situ* hybridization assays

Fluorescent in-situ hybridization assays were performed using the probes listed on Supplementary Table 7. FISH images were captured using the Metafer Slide Scanning Platform (MetaSystems, Altlußheim, Germany) and 200 non-overlapping tumor nuclei with at least 1 each signal were examined. Tumors with more than 20% nuclei with rearranged signals, fused or split depending on assays, were deemed rearrangement positive.

Targeted next-generation sequencing of cancer-related genes

Next-generation sequencing was performed using the NCC oncopanel test, which targets 114 cancer-associated genes, as described previously (1). Briefly, sections of FFPE samples were deparaffinized and subjected to DNA extraction using the DNA FFPE Tissue kit (Qiagen, Hilden, Germany). Sequencing libraries were prepared using the SureSelect XT reagent (Agilent Technologies, Santa Clara, CA, USA) and the KAPA Hyper Prep kit (KAPA Biosystems, Wilmington, MA, USA) and then analyzed on the NextSeq (Illumina) with 150 bp paired-end reads. Since non-tumor tissue samples were not available, single nucleotide polymorphisms were filtered out based on the following databases: 1000 Genomes (1 kgp, 201204) (http://www.1000genomes.org); the NHLBI GO Exome Sequencing Project (ESP6500) (http://evs.gs.washington.edu/EVS/); the Human Genetic Variation Database (HGVD, 20131010) (http://www.genome.med.kyoto-u.ac.jp/SnpDB); and the Integrative Japanese Genome Variation Database (iJGVD, 20151218) (https://ijgvd.megabank.tohoku.ac.jp/).

Immunohistochemistry

Immunohistochemical staining was performed for FFPE specimens. Antigen retrieval was performed using Target Retrieval Solution pH 9 (Agilent Technologies). The anti-N-terminal region of YAP1 antibody (dilution 1:200; clone 2F12; Abnova, Taipei, Taiwan), anti-C-terminal region of YAP1 antibody (dilution 1:200; clone D8H1X-XP;

Cell Signaling Technology, Beverly, MA, USA), and anti-NUTM1 antibody (dilution 1:200; clone C52B1; Cell Signaling Technology) were used as the primary antibodies. The anti-N-terminal region of YAP1 antibody cross-reacts with the N-terminal region of WWTR1 (2). For staining, we used an Autostainer Link 48 (Agilent Technologies) according to the manufacturer's protocol. An EnVision FLEX kit and Mouse LINKER (Agilent Technologies) were used for the detection. For evaluation of YAP1 staining, positive staining using N-terminal antibody in the absence of C-terminal antibody staining was considered a discordant expression pattern. For NUTM1 expression, any nuclear expression was deemed positive.

Plasmids

Plasmids containing cDNA for *YAP1* (FLJ84300AAAN), *WWTR1* (FLJ11974AAAF), *MAML2* (FLJ0462AAAN), and *NUTM1* (FLJ58711WAAN) (Biomedicinal Information Research Center, National Institute of Advanced Industrial Science and Technology, Tokyo, Japan) were used to construct the expression vectors. LATS1/2 kinase-resistant $YAP1^{S127A}$ and $YAP1^{5SA}$ were generated by in vitro mutagenesis so as to replace serine residues at 127 and 61/109/127/164/397, respectively, with alanine (3). $WWTR1^{S89A}$ and $WWTR1^{4SA}$ were similarly generated so as to replace serine residues at 89 and 66/89/117/311, respectively, with alanine (4). The fusion gene constructs were generated by using In-Fusion cloning kit (TAKARA, Kyoto, Japan). Some of the cDNA were fused to a 3x FLAG-tag sequence at the 5' end. The cDNA cloned in pENTR vector were recombined into pDEST-RetroX-TetOne-Puro, a destination vector based on pRetroX-tetOne-Puro (TAKARA).

Retrovirus infection

293T cells were obtained from Dr. Masao Seto, Kurume University, Fukuoka, Japan, and confirmed to express SV40 large T antigen. Retroviruses were produced by transfecting the retrovirus vectors together with packaging constructs pEF6-10A1 and pCL-Gag-Pol into 293T cells as described previously (5). NIH3T3 cells were provided by Dr. Masahide Takahashi, Nagoya University, Nagoya, Japan, and originally acquired from Dr. Geoffrey M Cooper (6). NIH3T3 cells were cultured in DMEM supplemented with 10% fetal bovine serum and infected with doxycycline-dependent inducible retrovirus vectors for expression of the respective transgenes. The infected

cells were selected in the presence of 1 μg/mL puromycin. Human dermal keratinocytes immortalized by lentivirus-mediated transduction of *TERT* and a mutant form of *CDK4* (referred to as HDK cells) were established and cultured under the conditions described previously (7). HDK cells were retrovirally transduced with MCAT8B-luc (a firefly luciferase reporter under the control of interferon-β minimum promoter with eight copies of the TEAD-binding MCAT motif：ACATTCCA), and a thymidine kinase promoter-driven Renilla luciferase expression construct. The resulting HDK cells harboring the TEAD reporter were further transduced with doxycycline-dependent inducible retrovirus vectors as described above.

TEAD luciferase reporter assay

The vector pMCAT8B-luc carries the firefly luciferase TEAD reporter as described above, while phRG-TK (Promega, Madison, WI, USA) carries the Renilla luciferase under the control of the thymidine kinase promoter (5). HEK293T cells were seeded on a 96-well plate at a density of 3 x 10^4 cells/well 1 day before transfection. The HEK293T cells were transfected with 50 ng pMCAT8B-luc, 10 ng phRG-TK, and 60 ng of individual pRetroX-tetOne-Puro plasmids encoding transgenes of interest in triplicate using polyethylenimine Max (Polysciences, Warrington, PA, USA). The cells were cultured in the presence or absence of 1 μg/mL doxycycline for 2 days and analyzed using Dual-luciferase reporter assay system (Promega). The HDK cells transduced with the TEAD reporter, the control Renilla luciferase, and individual doxycycline-inducible retrovirus vectors were seeded on a 96-well plate at a density of 1 x 10^4 cells/well in triplicate. The cells were cultured in the presence or absence of 1 μg/mL doxycycline for 3 days and analyzed using the Dual-luciferase reporter assay.

Immunofluorescence staining

HEK293T cells were seeded on 8-well chamber slide (Millipore, Bedford, MA, USA) at a density of 12,000 cells/well two days before transfection. Cells were transfected with 41 ng pRetroX-tetOne-Puro retroviral vector plasmid encoding 3x FLAG-tagged wild-type *YAP1*, *YAP1*^{S127A}, and *YAP1* fusions with polyethylenimine Max. The cells were incubated in the presence 1 μg/mL doxycycline for 3 days and fixed with 4% paraformaldehyde. Anti-FLAG M2 antibody (dilution 1:500; Sigma-Aldrich, St. Louis, MO, USA; F1804) was used as the primary antibody. Alexa Fluor 488-conjugated

Donkey anti-mouse IgG (dilution 1:500; ThermoFisher Scientific; A21202) was used for detection.

Immunoblotting

Whole-cell protein extracts were used for immunoblotting as described previously (8). Antibodies against the N-terminal region of YAP1 (clone 2F12), C-terminal region of YAP1 (clone D8H1X), WWTR1 (clone M2-616, BD Pharmingen, San Jose, CA, USA), NUTM1 (clone C52B1), GAPDH (Clone 6C5, ThermoFisher Scientific), and Vinculin (clone hVIN1, Sigma-Aldrich) were used as probes. Signals were detected by a LAS3000 imaging system (Fujifilm Co. Ltd., Tokyo, Japan).

Soft agarose colony formation assay

NIH3T3 and HDK cells transduced with doxycycline-dependent inducible retrovirus vectors were embedded in 0.4% SeaPlaque agarose (Lonza, Rockland, ME, USA) sandwitched by 0.7% agarose in 24-well plate and cultured with or without 1 μg/mL doxycycline for 2-3 weeks as described previously (9).

References

1. Sunami K, et al. Feasibility and utility of a panel testing for 114 cancer-associated genes in a clinical setting: A hospital-based study. *Cancer Sci.* 2019;110(4):1480-90.
2. Furukawa KT, Yamashita K, Sakurai N, and Ohno S. The Epithelial Circumferential Actin Belt Regulates YAP/TAZ through Nucleocytoplasmic Shuttling of Merlin. *Cell Rep.* 2017;20(6):1435-47.
3. Zhao B, et al. Inactivation of YAP oncoprotein by the Hippo pathway is involved in cell contact inhibition and tissue growth control. *Genes Dev.* 2007;21(21):2747-61.
4. Lei QY, et al. TAZ promotes cell proliferation and epithelial-mesenchymal transition and is inhibited by the hippo pathway. *Mol Cell Biol.* 2008;28(7):2426-36.
5. Yugawa T, et al. Regulation of Notch1 gene expression by p53 in epithelial cells. *Mol Cell Biol.* 2007;27(10):3732-42.

6. Takahashi M, Ritz J, and Cooper GM. Activation of a novel human transforming gene, ret, by DNA rearrangement. *Cell.* 1985;42(2):581-8.
7. Egawa N, et al. The E1 protein of human papillomavirus type 16 is dispensable for maintenance replication of the viral genome. *J Virol.* 2012;86(6):3276-83.
8. Nakahara T, et al. Activation of NF-kappaB by human papillomavirus 16 E1 limits E1-dependent viral replication through degradation of E1. *J Virol.* 2015;89(9):5040-59.
9. Narisawa-Saito M, et al. An in vitro multistep carcinogenesis model for human cervical cancer. *Cancer Res.* 2008;68(14):5699-705.

Supplemental Figures

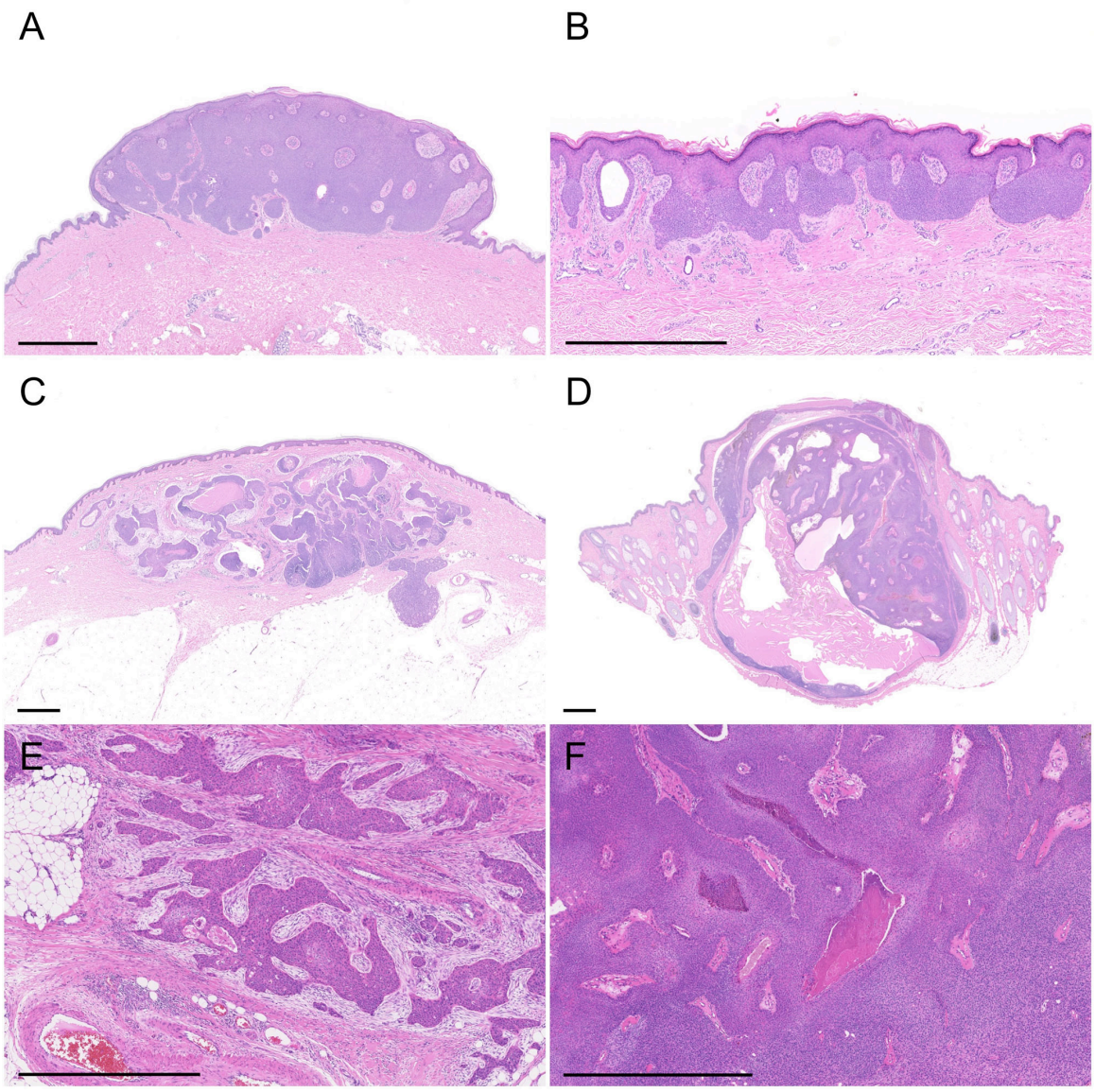

Supplemental Figure 1: Representative histology of poroma subtypes and porocarcinoma

A: Poroma, representing the most common subtype. An elevated lesion consisting of tumor cell proliferation in broad continuity with the epidermis. **B:** Hidroacanthoma simplex. Tumor cells are confined to the epidermal layer. **C**: Dermal duct tumor. Tumor nests are primarily confined to the dermis without apparent connection to the epidermis. **D**. Poroid hidradenoma. A discrete solid and cystic nodule centered on the dermis. **E**: Porocarcinoma. Infiltrative tumor nests associated with fibrous stroma. **F**: Poroma with necrotic foci. Scale bars, 1 mm.

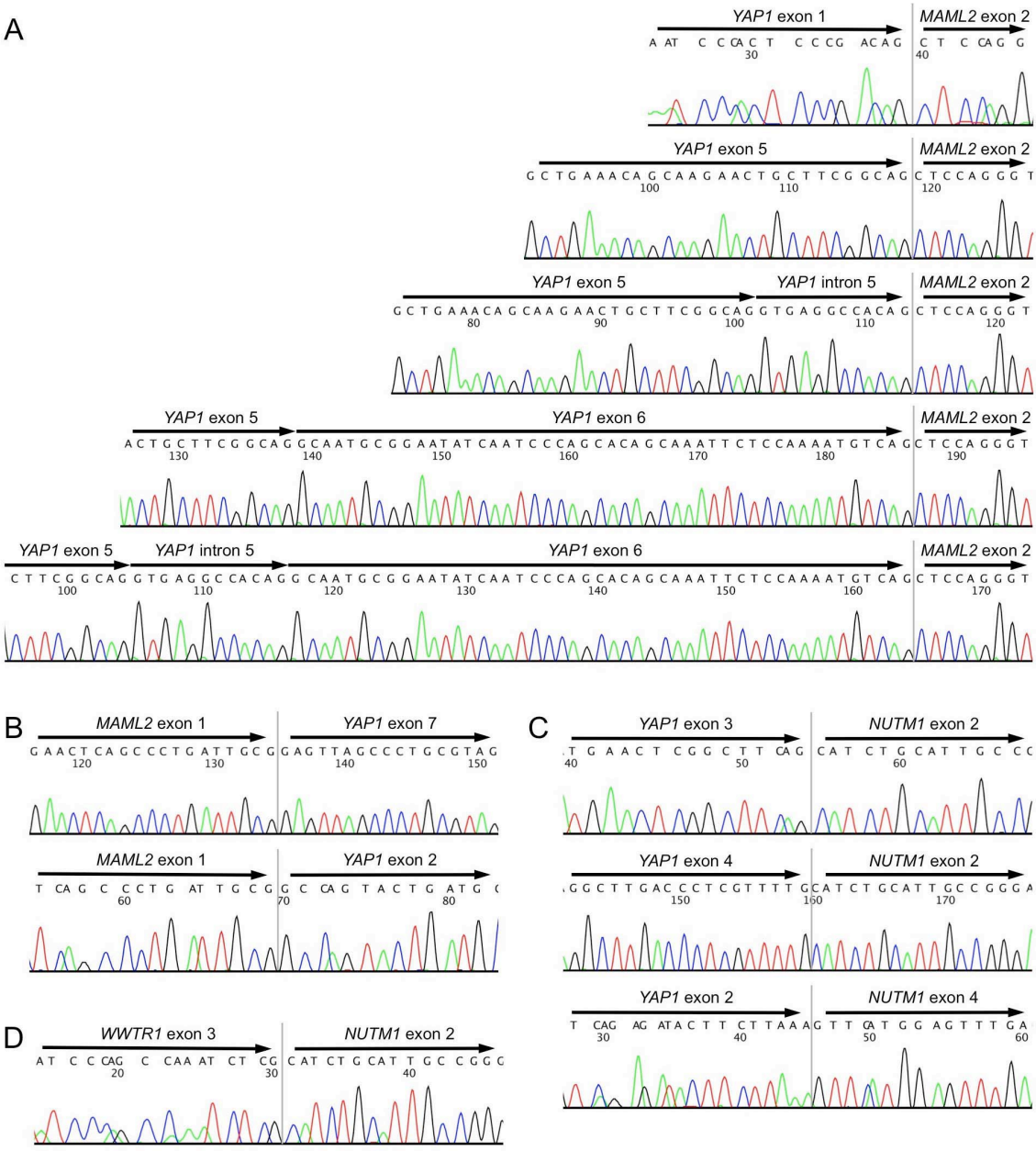

Supplemental Figure 2: Sanger sequencing of *YAP1* and *WWTR1* fusion junctions **A**: *YAP1-MAML2* fusions. *YAP1* exon 5-*MALM2* and *YAP1* exon 6-*MAML2* fusions with or without 12-bp intronic sequences were concurrently detected in many of the lesions. **B**: *MAML2-YAP1* fusions. These were consistently associated with the reciprocal *YAP1-MAML2* fusions. **C**: *YAP1-NUTM1* fusions. **D:** *WWTR1-NUTM1* fusion. Vertical bars indicate fusion junctions. All the fusion transcripts were in-frame.

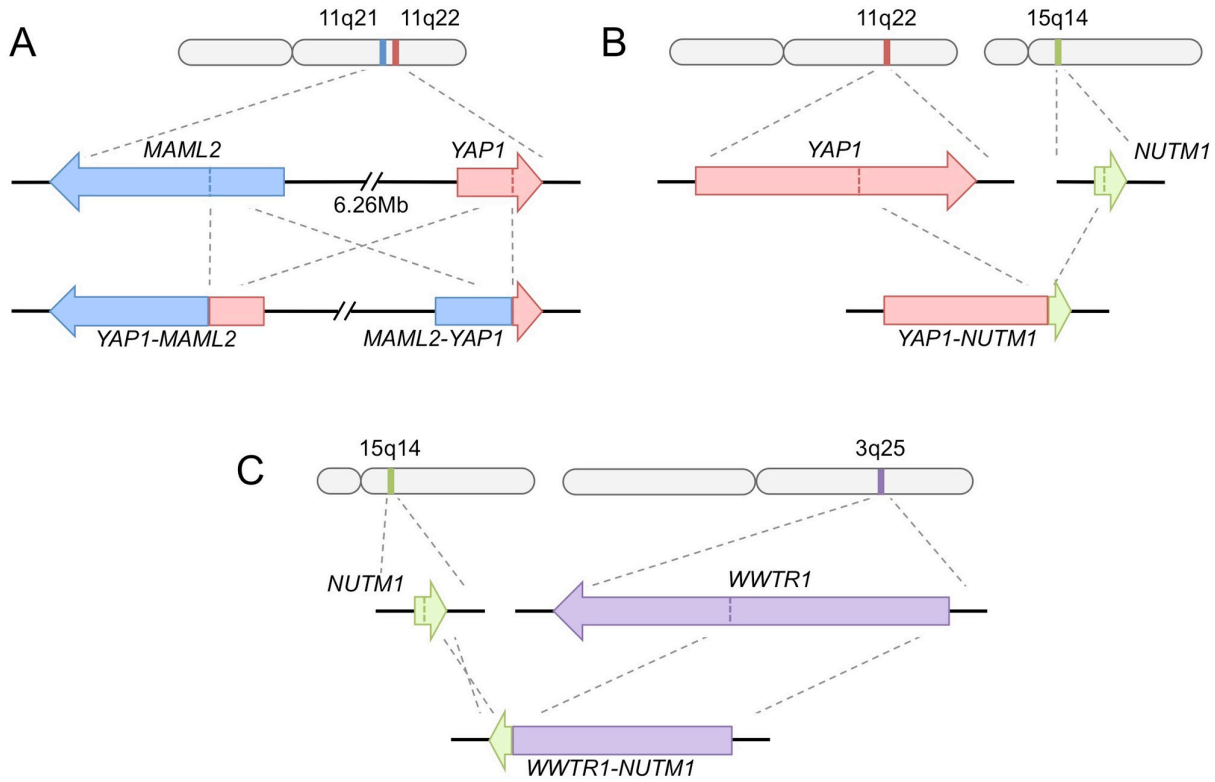

Supplemental Figure 3: Expected genomic structures underlying *YAP1* and *WWTR1* fusions

A: The close localization of *YAP1* and *MAML2* and the common presence of reciprocal *YAP1-MAML2* and *MAML2-YAP1* fusions imply intrachromosomal inversion as a major cause of these fusions. **B**, **C**: *YAP1-NUTM1* and *WWTR1-NUTM1* fusions are thought to result from interchromosomal translocations.

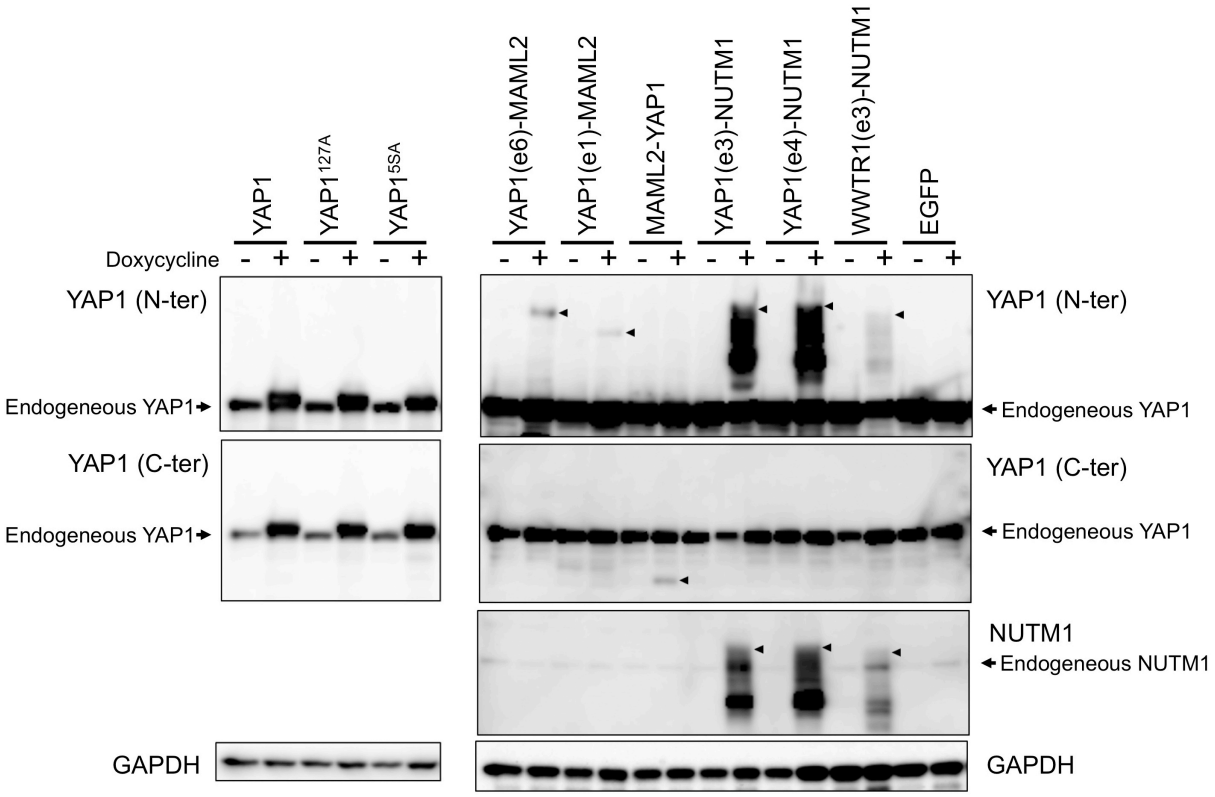

Supplemental Figure 4: Expression of fusion transgene products in NIH3T3 cells NIH3T3 cells transduced with doxycycline-dependent inducible retroviruses were cultivated with or without 1 μg/mL doxycycline. Whole-cell extracts were analyzed by immunoblotting with the indicated antibodies. Fusion gene products were detected using anti-YAP1 antibodies specific to the N-terminal (N-ter) or C-terminal region (C-ter). The expression of YAP1-NUTM1 and WWTR1-NUTM1 fusions was also detected by an anti-NUTM1 antibody. Arrowheads indicate the expected molecular weights of fusion products. Note that the WWTR1-NUTM1 fusion was also detected by an antibody against N-terminal region of YAP1 with its known cross-reactivity.

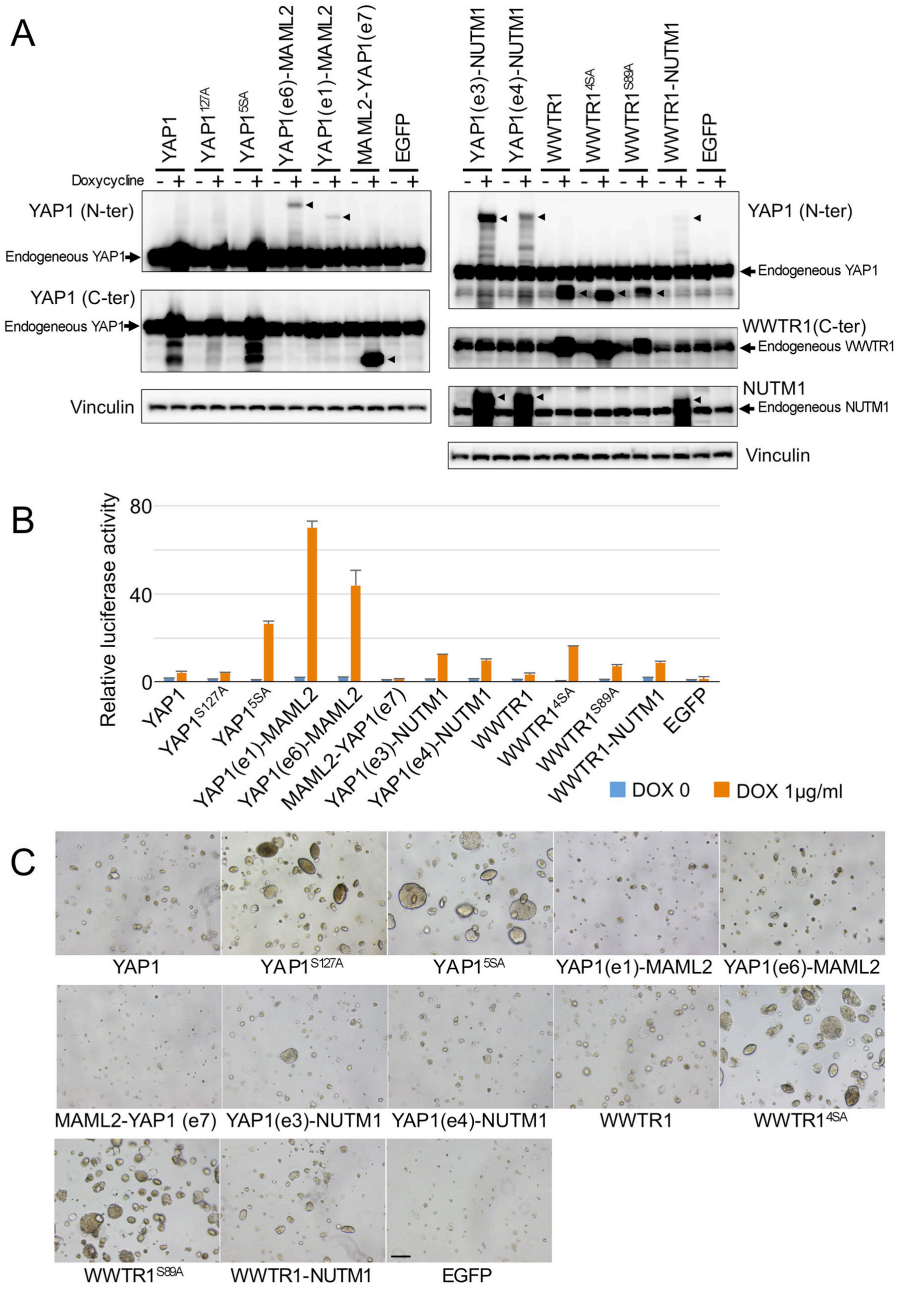

Supplemental Figure 5: TEAD luciferase reporter and soft agar colony formation assays in human dermal keratinocyte cell lines

A: HDK cells retrovirally transduced with a TEAD reporter and doxycycline-dependent inducible transgenes were cultivated with or without 1 µg/mL doxycycline. Whole-cell extracts were analyzed by immunoblotting with the indicated antibodies. Fusion gene products were detected using anti-YAP1 N-terminal (N-ter), anti-YAP1 C-terminal (C-ter), anti-NUTM1, or anti-WWTR1 antibodies. Arrowheads indicate the expected

molecular weights of the fusion products. Note that the mutant WWTR1 and WWTR1 fusion gene products were also detected by anti-YAP1 N-terminal antibody due to its cross-reactivity. **B**: TEAD luciferase reporter assays performed HDK cells transduced with doxycycline-inducible vectors. *YAP1*^{S127A}, *YAP1*^{5SA}, *WWTR1*^{4SA}, and *WWTR1*^{S89A} represent constitutively active mutants. The luciferase activity of EGFP-transfected cells in the absence of doxycycline is set at 1 to indicate relative luciferase activities. Data represent mean of triplicate measurements ± SD. **C**: Soft agar colony formation assay of HDK cells expressing the fusion transgenes. HDK cells transduced with doxycycline-dependent inducible retrovirus vectors were subjected to a soft agar colony formation assay in the presence of doxycycline. At day 14, HDK cells transduced with constitutively active YAP1 and WWTR1 mutants formed large colonies whereas those transduced with wild-type YAP1, WWTR1, YAP1 fusions, and WWTR1 fusions formed small colonies. No colony formation was observed in cells transduced with either MAML2-YAP1 fusion or EGFP. None of the clones formed colonies in the absence of doxycycline. Scale bar, 200 μm

Supplemental Tables

Supplemental Table 1: *YAP1* and *WWTR1* fusions detected by RNA sequencing

Case#	Gene 1	Position 1	Strand 1	Gene 2	Position 2	Strand 2	Paired Read	Split Read
6	*MAML2*	chr11:96,074,546	-	*YAP1*	chr11:102,094,352	+	1	14
6	*YAP1*	chr11:102,076,802	+	*MAML2*	chr11:95,826,681	-	2	6
7	*MAML2*	chr11:96,074,546	-	*YAP1*	chr11:102,094,352	+	0	6
7	*YAP1*	chr11:102,076,802	+	*MAML2*	chr11:95,826,681	-	0	9
8	*MAML2*	chr11:96,074,546	-	*YAP1*	chr11:102,094,352	+	2	12
8	*YAP1*	chr11:102,076,802	+	*MAML2*	chr11:95,826,681	-	6	8
12	*MAML2*	chr11:96,074,546	-	*YAP1*	chr11:102,094,352	+	1	2
12	*YAP1*	chr11:102,076,802	+	*MAML2*	chr11:95,826,681	-	0	5
62	*WWTR1*	chr3:149,290,651	-	*NUTM1*	chr15:34,640,169	+	33	49
66	*YAP1*	chr11:102,033,299	+	*NUTM1*	chr15:34,640,167	+	27	33
67	*YAP1*	chr11:102,056,861	+	*NUTM1*	chr15:34,640,169	+	38	42
167	*YAP1*	chr11:102,056,861	+	*NUTM1*	chr15:34,640,169	+	22	17

Supplemental Table 2: Clinicopathological features of poroma and porocarcinoma

		Poroma (n = 104)	Porocarcinoma (n = 11)
Age, year-old (median, range)		67, 27-93	75, 53-92
Sex (male/female)		63/41	6/5
Size, mm* (median, range)		8, 3-45	30, 8-47
Site	Head and neck	22	5
	Trunk	26	4
	Extremities	56	2
Histological subtype	Poroma	91	
	Hidroacanthoma simplex	5	
	Dermal duct tumor	2	
	Poroid hidradenoma	6	

*, excluding samples obtained by biopsy

Supplemental Table 3: Fluorescent *in-situ* hybridization (FISH) analysis results

Case#	Histology	Fusion transcripts	FISH results			
			YAP1-5'/ *YAP1*-3'	*NUTM1*-5'/ *NUTM1*-3'	*YAP1*-5'/ *MAML2*-3'	*YAP1*-5'/ *NUTM1*-3'
177	Poroma	*YAP1* (e1)-*MAML2*	Split	ND	ND	ND
186	Poroma	*YAP1* (e1)-*MAML2*	Isolated 5'	ND	ND	ND
168	Porocarcinoma	*YAP1* (e1)-*MAML2*	Isolated 5'	ND	ND	ND
70	Poroma	*YAP1* (e1)-*MAML2*, *MAML2*-*YAP1* (e2)	Split	ND	Fused	ND
178	Poroma	*YAP1* (e1)-*MAML2*, *MAML2*-*YAP1* (e2)	Split	ND	Fused	ND
210	Poroma	*YAP1* (e5)-*MAML2*, *MAML2*-*YAP1* (e7)	Split	ND	Fused	ND
223	Poroma	*YAP1* (e5)-*MAML2*, *MAML2*-*YAP1* (e7)	Split	ND	ND	ND
58	Poroma	*YAP1* (e5/6)-*MAML2*, *MAML2*-*YAP1* (e7)	Split	ND	ND	ND
63	Poroma	*YAP1* (e5/6)-*MAML2*, *MAML2*-*YAP1* (e7)	Split	ND	Fused	ND
65	Poroma	*YAP1* (e5/6)-*MAML2*, *MAML2*-*YAP1* (e7)	Split	ND	Fused	ND
69	Poroma	*YAP1* (e5/6)-*MAML2*, *MAML2*-*YAP1* (e7)	-	-	ND	ND
71	Poroma	*YAP1* (e5/6)-*MAML2*, *MAML2*-*YAP1* (e7)	Split	ND	Fused	ND
173	Poroma	*YAP1* (e5/6)-*MAML2*, *MAML2*-*YAP1* (e7)	Split	-	Fused	ND
206	Poroma	*YAP1* (e5/6)-*MAML2*, *MAML2*-*YAP1* (e7)	Split	ND	Fused	ND
211	Poroma	*YAP1* (e5/6)-*MAML2*, *MAML2*-*YAP1* (e7)	Split	ND	Fused	ND
215	Poroma	*YAP1* (e5/6)-*MAML2*, *MAML2*-*YAP1* (e7)	Split	ND	Fused	ND
60	Poroma	*YAP1* (e3)-*NUTM1*	Split	Split	-	Fused
66	Poroma	*YAP1* (e3)-*NUTM1*	Split	Isolated 3'	ND	Fused
185	Poroma	*YAP1* (e3)-*NUTM1*	Split	Split	ND	Fused
197	Poroma	*YAP1* (e3)-*NUTM1*	ND	Split	ND	ND
202	Poroma	*YAP1* (e3)-*NUTM1*	ND	Split	ND	ND
19	Porocarcinoma	*YAP1* (e3)-*NUTM1*	Split	Split	ND	Fused
55	Porocarcinoma	*YAP1* (e3)-*NUTM1*	Split	Split	ND	Fused
232	Porocarcinoma	*YAP1* (e3)-*NUTM1*	ND	Split	ND	Fused
67	Poroma	*YAP1* (e3/4)-*NUTM1*	Split	Split	ND	Fused
163	Poroma	*YAP1* (e3/4)-*NUTM1*	Split	Split	ND	Fused
207	Poroma	*YAP1* (e3/4)-*NUTM1*	ND	Split	ND	Fused
212	Poroma	*YAP1* (e3/4)-*NUTM1*	ND	Split	ND	ND
218	Poroma	*YAP1* (e3/4)-*NUTM1*	ND	-	ND	ND
221	Poroma	*YAP1* (e3/4)-*NUTM1*	ND	Split	ND	Fused
62	Poroma	*WWTR1*-*NUTM1**	-	Split	ND	ND
169	Poroma	Negative	-	ND	-	-
196	Porocarcinoma	Negative	-	-	ND	ND

*, The poroma with a *WWTR1-NUTM1* fusion (case 62) showed split signals for *WWTR1*-5'/*WWTR1*-3' and fusion signals for *WWTR1*-5'/*NUTM1*-3'

ND, not done; -, no rearrangement

Supplemental Table 6: Primers for RT-PCR

Target	Forward primer	Reverse primer
YAP1 (e5/6)-*MAML2* (e2)	CAACTGCAGATGGAGAAGGAGAG	GCTTGCTGTTGGCAGGAGATAG
YAP1 (e6)-*MAML2* (e2)	TCAATCCCAGCACAGCAAATTC	ATTGGGTCGCTTGCTGTTGG
MAML2 (e1)-*YAP1* (e7)	GTGGTGGGATAAACGGAGAGC	CCTGCTCCAGTGTTGGTAAC
YAP1 (e1)-*MAML2* (e2)	GAAGCTGCCCGACTCCTTCTT	TTGCTGTTGGCAGGAGATAGG
MAML2 (e1)-*YAP1* (e2)	ATAATGGTGGCAGTGGTGGG	CTGCAGTGCCTGCATCAGTA
YAP1 (e3)-*NUTM1* (e2)	CCATGCTGTCCCAGATGAAC	AGGTTTCATGCTCATATCCGGT
YAP1 (e4)-*NUTM1* (e2)	AAACCATAAGAACAAGACCACCTC	GGGGCGGCACTAGGTTT
YAP1 (e2)-*NUTM1* (e4)	CCTGATGATGTACCTCTGCC	GAATCTGCATCTCCTCAGCCT
WWTR1 (e3)-*NUTM1* (e2)	CGTCAGTTCCACACCAGTGC	GGGGCGGCACTAGGTTTCAT
ACTB	CCTCGCCTTTGCCGATCC	CTCGTCGCCCACATAGGAAT

Supplemental Table 7: Probes for FISH analyses

Target	Position (hg19)/BAC clone	Vendor
YAP1-5'	chr11:101,695,525-102,095,619	Agilent Technologies, Palo Alto, CA, USA
YAP1-3'	chr11:102,210,220-102,608,504	Agilent Technologies
MAML2-3'	chr11:95,426,979-95,826,198	Agilent Technologies
NUTM1-3'	chr15:34,642,579-35,192,873	Agilent Technologies
WWTR1-5'	chr3:149,389,615-149,789,909	Agilent Technologies
WWTR1-3'	chr3:148,889,795-149,289,894	Agilent Technologies
NUTM1-5' (BAC)	RP11-412E10	Chromosome Science Labo Inc., Sapporo, Japan
NUTM1-3' (BAC)	RP11-1H8	Chromosome Science Labo Inc.